NSG-639

PART II

EFFECT OF Ti, Zr, AND C ON STRUCTURE AND PROPERTIES OF A Co-35W-3Cr-0.1B ALLOY

by

S. F. Ramseyer* and J. F. Wallace**

*Presently with General Electric Company, Knolls Atomic Power Laboratory

**Professor of Metallurgy, Metallurgy Department, Case Western Reserve University.

ABSTRACT

An investment cast alloy of base composition Co-35W-3Cr-0.1B was used to study the interactions of Ti, Zr, and C in determining structure and stress rupture properties at 1850°F in air.

The atomic ratio of Ti plus Zr to C affected both the type and morphology of the second phases that formed. As the ratio increased from 0 to approximately 1/2, a continuous network of M_6C carbides with increased MC carbides occurred; above 1/2 to 1 the M_6C network was broken up, the particles becoming rounder and more equiaxed, and an increasing percent of MC carbides formed; and above 1, MC carbides and a new phase were observed.

The atomic ratio of Ti and Zr to C also affected stress rupture properties considerably. Optimum results were obtained with a ratio of .76. Two alloys based on this ratio, Co-35W-3Cr-0.1B with additions of 1Ti-1Zr-0.5C and 2Ti-2Zr-1C had stress rupture lives which compare very favorably with commercial Co-base alloys.

INTRODUCTION

In a previous phase of research at Case on "Modified Eutectic Alloys for High Temperature Service" under NASA Grant NsG-639, considerable attention was devoted to a Co-35W base composition (1). The beneficial influences of Ti, Zr, C and Cr were established; however, Mo, V, Ta + Nb and N_2 additions failed to produce this improvement. This work resulted in the development of several Co-35W base alloys exhibiting excellent stress rupture behavior in air at 1850°F. These results have been described in detailed form (1).

An additional limited study was conducted on the interaction of Ti, Zr, and C in a base alloy of Co-35W-3Cr-0.1B. The results of this work were not available for inclusion in the second annual report for the contract period May 1965 to June 1966 and are being presented here as a supplement to that investigation.

PROCEDURE

The nominal compositions of the Co-35W-3Cr-0. 1B base alloys investigated are listed in Table I. These alloys werevaccum induction melted and poured under a pressure of 1/2 atmosphere of argon into ceramic investment molds to produce cast to size stress rupture specimens. The melting and casting procedure has been described in detail in the second annual report (1).

Constant load stress rupture tests were conducted in air at 1850°F. Both ductility, as reduction in area, and rupture life were determined in these tests.

Metallographic examination was performed on both as cast and tested stress rupture specimens. The mechanically polished structures were etched with a modified Fry's etch consisting of 50cc HCl, 25cc HNO_3, 1 gram $CuCl_2 \cdot 2H_20$, and 150cc H_20.

RESULTS AND DISCUSSION

Microstructural Considerations

Figures 1-9 show the microstructures of alloys cast to determine the specific influence of Ti, Zr and C on the cast structure and properties of a Co-35W-3Cr-0.1B base alloy, Photomicrographs marked "after-testing" are of samples cut from the gage length of specimens tested in air at 1850°F and 20,000 psi initial load. The structure of these alloys etched more readily and for this reason these structures usually appear darker. The atom ratio of the Ti + Zr to C added was shown to have a major influence on both the types and morphology of phases which occurred in the as cast structures. A continuous interdendritic network of the M_6C carbide, Co_3W_3C or η phase in a "chinese script" pattern, formed when only C was added to the base alloy, as shown in Figures 1 and 5. The morphologies of the M_6C were similar in the two alloys, with the volume percent of the carbide phase increasing approximately 50% as the C level was raised from 0.5 to 1. The considerably finer dendritic structure for the 0.5C alloy resulted because of the lower pouring temperature for this heat, 150°F superheat compared to the usual 300°F. With the addition of Ti, Zr and C in a ratio less than approximately 0.5

as exemplified by the alloys with 2Zr-1C and 2Ti-1C, Figures 6 and 7 respectively, the M_6C network is still continuous though reduced in volume. The MC's have formed in varying amounts and are present in greater amounts in the 2Ti-1C alloy with a ratio of 0. 5 than in the 2Zr-1C alloy with a ratio of 0. 26.

By increasing the ratio beyond 0. 5, the M_6C network is partially or completely broken up. At a ratio of 0. 53 for the 2Zr-0. 5C alloy, the M_6C particles are only partly dispersed, Figure 2. At a ratio of 0.76, as for the 1Ti-1Zr-0. 5C alloy in Figure 8 and the 2Ti-2Zr-1C alloy in Figure 9, the M_6C network is completely broken up with faceted particles of the MC carbides randomly mixed with the fine, equiaxed M_6C carbide particles. The only differences between the two structures are the slight increase in the volume percent of second phases and the larger, more idiomorphic MC particles in the latter alloy.

If the ratio is increased still further to a stoichiometric addition of Ti + Zr to C of 1, as illustrated by the 2Ti-0. 5C alloy shown in Figure 3, the structure has a very high percentage of MC carbides and only a few random particles of a third phase that is assumed to be the M_6C. With the increase in the ratio to approximately 1. 5 for the 2Ti-2Zr-0. 5C alloy shown in Figure 4, a large excess of Ti + Zr exists and a bulky new phase forms,

probably a $(Ti, Zr)Co_3$ compound (2). Interspersed with these were smaller faceted particles, probably MC carbides. However, these phases were not definitely established.

At agiven C level the MC carbides will form at the expense of the M_6C carbides, since these are the more stable phase thermodynamically. Since the molar volume of the M_6C phases would be expected to be considerably larger than that for the MC phases, the decrease in the volume fraction of the second phases observed with an increasing Ti + Zr to C ratio (see Table II) at a constant C level probably reflects this change in the amounts of M_6C and MC phases formed.

The variation in as cast grain size of this series of alloys, as presented in Table 11, was very erratic. The majority of the alloys had a grain size of from 10-15 grains per 1/4 inch diameter for the 0. 5C alloy was probably due to the lower pouring temperature of this heat; the cause of the very small grain size of approximately 40 grains per diameter for the 2Ti-0, 5C could not be definitely established. Titanium is known to be a very effective grain refiner for certain cast steels (3) and perhaps, when added singularly to this Co-base alloy, it acts in a similar manner. It should also be noted that the grain size of 2-4 and 6-8 grains per diameter for the two heats of the 2Ti-2Zr-1C alloy was slightly

coarser than for the other alloys.

The influence of Ti, Zr and C on the microstructure of the Co-35W-3Cr-0. 1B base alloy after exposure to 1850°F is shown by comparing the various "after-testing" microstructures. When the M_6C carbide was a continuous interdendritic network, Figures 1, 5-7, no noticeable precipitation of the Co_3W phase was evident in the "after-testing" structures. The amount and coarseness of the Co_3W precipitation after exposure at 1850°F increased as the Ti+Zr to C ratio was increased as indicated by the "after-testing" structures presented in Figures **2-4,** 9. The structures of these latter alloys exhibited smaller amount of M_6C, larger amounts of the MC phases and a broken up M_6C network. The morphology and size of the carbide phases were generally unchanged after testing at 1850°F. The differences in response of the matrices to exposure to elevated temperatures is probably caused by the influence of Ti and Zr on the amount of W in solid solution in the Co matrix. Without the addition of Ti and Zr, sufficient W is tied up by the formation of the M_6C phase network to lower the W dissolved in the matrix below the level at which Co_3W will form and precipitate at 1850°F. This appears to be true as long as the M_6C carbide network is continuous. However, when the Ti plus Zr level is increased to the level where the M_6C carbide network is broken up, i.e., carbon

is tied up as MC and the M_6C does not form in as large quantities, the matrix becomes supersaturated in W, and Co_3W precipitates during testing at 1850°F. The progressive coarsening of the matrix precipitate with increasing Ti+Zr to C ratio is shown by comparing the "after-testing" structures illustrated in Figures 2-4. The particularly heavy precipitation noted in the 2Ti-2Zr-1C alloy (Figure 9) was probably caused in part by the longer time at elevated temperature.

Stress Rupture Properties of Co-35W Base Alloys

The stress rupture curves for the various alloys tested are presented in Figures 10 and 11. Table III lists both time to fracture and reduction in area at the different levels of initial stress. The calculation of reduction in area was questionable in some cases because of the anisotropic nature of the fracture cross section or extensive oxidation of the test specimen. These values have been marked either (a) or (o) in Table III.

The results of the investigation into the effect of Ti, Zr and C additions to a Co-35W-3Cr-0.1B base material are presented by separating the alloys into two groups by C level: 0.5C level alloys shown in Figure 10 and 1.0C level alloys in Figure 11, The two alloys with only C added had the poorest stress rupture lives, as would be expected from the continuous interdendritic

carbide network in their microstructures (Figures 1 and 5). Although these alloys exhibited extensive void formation and cracking along the full gage length after testing, both had substantial ductility, approximately 50% reduction in area for the alloy with 0.5C and 20-25% reduction in area for the alloy with 1.0C. The large reductions in area for the alloys during stress rupture testing is probably caused by the effect of the carbide network on the W content and distribution in the Co matrix. With the formation of a continuous network of the M_6C sufficient tungsten is tied up so Co_3W cannot form during testing and a low W zone probably exists near the matrix-carbide interface. Thus, the matrix and particularly the interface is relatively weak so extensive deformation and grain boundary sliding occurred. The extensive interface deformation would also account for the larger number of voids and cracks which formed during the testing of these alloys.

The atomic ratio of Ti + Zr to C was found to be a more significant factor in correlating the influence of alloy content on properties than either weight or atomic percent of Ti, Zr and/or C added, As the ratio increased the stress rupture life increased initially, then decreased when the ratio was equal to or greater than one. The importance of the ratio probably results from its effect on the type of carbides and morphology that forms. As the

ratio increases from 0 to about 1/2, the continuous network of the M_6C carbide forms in increasingly smaller amounts and finer size, with a certain amount of MC carbides occurring. The properties for the 2Zr-1C (ratio-0. 26) and 2Ti-1C (ratio 0. 50) alloys shown in Figure 11 illustrate the influence of these changes in microstructure. The modest improvement in properties for the 2Zr-1C alloy above those for the 1C alloy is probably caused by the tying up of some of the C as ZrC. Thus, less M_6C forms, more W is in solid solution, so the matrix and particularly the interface region is strengthened. Further improvement in properties resulted when more C is tied up in the 2Ti-1C alloy. Both of these alloys had substantial elevated temperature ductility (reductions in area of approximately 40-50%) with void and crack formation along the full gage length. This behavior is similar to that observed for the 1C alloy.

As the ratio increases further from 1/2 to 1, the M_6C network is broken, the particles become more rounded and equiaxed and appear in decreasing amounts, and the MC carbides increase in amount and size. These changes in microstructure are reflected in the slightly improved properties for the 2Zr-0. 5C and 2Ti-0. 5C alloys at 20, 000 psi, Table 111. The analysis of these alloys is complicated by the observed accelerated oxidation for the 2Zr-0. 5C alloy, and the very fine grain size of the 2Ti-0. 5C alloy.

Both these factors tend to lower the stress rupture properties of a material by causing premature failures at lower stress levels, and longer testing times. Thus, the improved life of both these alloys at the higher stress of 20, 000 psi is nullified at the lower stress of 15,000 psi and the slopes to their stress rupture curves are steeper, Figure 10. At still higher ratios, with Ti + Zr in excess of the stoichiometric amount needed to form the MC carbides, a new phase forms which weakens the material. The detrimental effect of excess Ti + Zr is shown by comparing the stress rupture curve of the 2Ti-2Zr-0. 5C alloy (ratio 1. 53) with that of the standard 1Ti-1Zr-0. 5C (ratio . 76) in Figure 10.

A ratio slightly less than one appears to be optimum judging by the excellent properties of the standard and Co-35W-3Cr-2Ti-2Zr-IC-0. 1B alloys, both with ratios of 0.76. The better properties of the latter over the former shows the effect of increased amounts of Ti, Zr and C and indicates that still larger additions might increase stress rupture life further. A point of diminishing returns exists because the structure becomes overloaded with carbides and the oxidation rate increases at higher Ti and Zr contents.

The stress rupture properties of the Co-35W base alloys developed in this study are compared with a number of commercial Co-base alloys in Figures 12 and 13. The best alloy developed,

Co-35W-3Cr-2Ti-2Zr-1C-0.1B compared favorably with commercial alloys of this type when compared on a strength to weight basis.

SUMMARY

Using a base alloy of Co-35W-3Cr-0.1B, it was found that the atomic ratio of Ti + Zr to C determined both the type and morphology of the second phases that formed. As the ratio increased from 0 to approximately 1/2, a continuous network of M_6C carbides with increased MC carbides occurred; above 1/2 to 1 the M_6C network was broken up, the particles becoming rounder and more equiaxed, and an increasing percent of MC carbides formed; and above 1, MC carbides and a new phase were observed.

The atomic ratio of Ti and Zr to C also affected stress rupture properties considerably. Optimum results were obtained with a ratio of .76. Two alloys based on this ratio, Co-35W-3Cr-0.1B with additions of 1Ti-1Zr-0.5C and 2Ti-2Zr-1C had stress rupture lives which compare very favorably with commercial Co-base alloys.

LIST OF REFERENCES

1. S. F. Ramseyer and J. F. Wallace, "Second Year Interim Technical Report on NASA Grant Sc-NsG-639", June 1966.

2. H. T. Wagner and A. M. Hall, "The Physical Metallurgy of Cobalt-Base Superalloys" DMIC Rpt. 171 AF 33 (616)-7747, July 6, 1962, Columbus, Ohio.

3. N. Church, P. Wieser and J. F. Wallace, "Control of Cast Grain Size of Steel Castings, Effect of Grain Refinement and Properties", Trans. AFS., Vol. 74, 1966, pp. 113-128.

4. J. C. Freche, R. L. Ashbrook and G. D. Sandrock, "The Potential for Cobalt-Tungsten Superalloys", Metal Progress, May 1965, p. 74.

5. H. L. Wheaton, MAR-M-509, "A New Cast Cobalt-Base Alloy for High Temperature Service", Cobalt, Vol. 29, December 1965, p. 163.

TABLES

TABLE I

NOMINAL COMPOSITION OF ALLOYS INVESTIGATED

(Weight Percent)

Co-35W-3Cr-0.5C-0.1B

Co-35W-3Cr-2Ti-0.5C-0.1B

Co-35W-3Cr-2Zr-0.5C-0.1B

Co-35W-3Cr-2Ti-2Zr-0.5C-0.1B

Co-35W-3Cr-1C-0.1B

Co-35W-3Cr-2Ti-1C-0.1B

Co-35W-3Cr-2Zr-1C-0.1B

Co-35W-3Cr-1Ti-1Zr-0.5C-0.1B

Co-35W-3Cr-2Ti-2Zr-1C-0.1B

TABLE II

QUANTITATIVE METALLOGRAPHIC DATA FOR SEVERAL Co-35W BASE ALLOYS

Alloy Composition (Niminal-Wt. %)	Atomic Ratio Ti+Zr/C	Grain Size, Grains per 1/4"-Dia.	Total Vol. Fraction of Second Phases	Mean Free Path Microns	Time to Fracture at 1850°F and 15,000 psi, Hrs.
Co-35W-3Cr-1Ti-1Zr-0.5C-0.1B					
a)	.76	7-10	21.0	20.1	154.2
b)	.76	12-16	20.8	21.2	131.9
c)	.76	9-12	20.1	19.9	144.3
d)	.76	15-20	21.0	20.7	150.7
Co-35W-3Cr-0.5C-0.1B	0	15-20	32.5	10.8	6.3
Co-35W-3Cr-2Zr-0.5C-0.1B	.53	8-12	28.5	24.2	35.7
Co-35W-3Cr-2Ti-0.5C-0.1B	1.0	40	22.1	24.4	31.3
Co-35W-3Cr-2Ti-2Zr-0.5C-0.1B	1.5	10-15	21.8	27.2	46.0
Co-35W-3Cr-1C-0.1B	0	10-15	48.0	21.4	1.4
Co-35W-3Cr-2Zr-1C-0.1B	.26	10-15	37.0	26.5	8.1
Co-35W-3Cr-2Ti-1C-0.1B	.50	10-15	36.0	28.8	5.8
Co-35W-3Cr-2Ti-2Zr-1C-0.1B					
a)	.76	2-4	24.0	19.3	224.9
b)	.76	6-8	22.5	17.4	171.7

TABLE III

RESULTS OF STRESS RUPTURE TESTS IN AIR AT 1850° F

Alloy Composition (Nominal-Wt. %)	Initial Stress psi	Time to Fracture Hours	Reduction in Area Percent	
Co-35W-3Cr-1Ti-1Zr-0.5C-0.1B[a]	15,000	145.2	-	(o)
	17,500	61.7	-	
	20,000	29.5	-	
	22,500	17.6	-	
	25,000	11.5	-	
Co-35W-3Cr-0.5C-0.1B	15,000	6.3	51.8	
	17,500	3.3	55.2	
	20,000	2.0	46.3	
Co-35W-3Cr-2Zr-0.5C-0.1B	15,000	35.7	89.7	(o)
	17,500	19.3	69.6	(o)
	20,000	12.0	84.6	(o)
Co-35W-3Cr-2Ti-0.5C-0.1B	15,000	31.3	37.2	
	17,500	18.5	39.1	
	20,000	13.2	30.9	
Co-35W-3Cr-2Ti-2Zr-0.5C-0.1B	15,000	46.0	18.2	
	17,500	28.5	30.8	
	20,000	23.0	16.2	
Co-35W-3Cr-1C-0.1B	15,000	1.4	29.8	
	17,500	0.7	14.8	
	20,000	0.3	46.0	
	20,000	0.4	15.1	
Co-35W-3Cr-2Zr-1C-0.1B	15,000	8.1	40.0	
	17,500	5.4	40.0	
	20,000	2.3	23.0	

(A) Anistropic deformation, assumed ellipsoidal fracture cross-section

(o) Heavy Oxidation

[a] Average of 5 heats. Heats listed individually, Table VI (Ref. 1).

TABLE III (continued)

Alloy Composition (Nominal-Wt. %)	Initial Stress psi	Time to Fracture Hours	Reduction in Area Percent
Co-35W-3Cr-2Ti-1C-0.1B	15,000	36.1	55.7
	17,500	12.8	65.2
	20,000	5.8	26.8
Co-35W-3Cr-2Ti-2Zr-1C-0.1B	15,000	224.9	29.2(A)(o)
	15,000	171.7	22.2(A)(o)
	17,500	117.1	37.8
	17,500	70.7	24.4
	20,000	44.8	34.8
	25,000	14.9	28.9
Co-35W-3Cr-1Ti-1Zr-0.5C	15,000	52.0	7.0
	17,500	29.8	2.5
	20,000	20.4	4.8
	25,000	8.0	8.7

(A) Anistropic deformation, assumed ellipsoidal fracture cross-section.
(o) Heavy Oxidation.

FIGURES

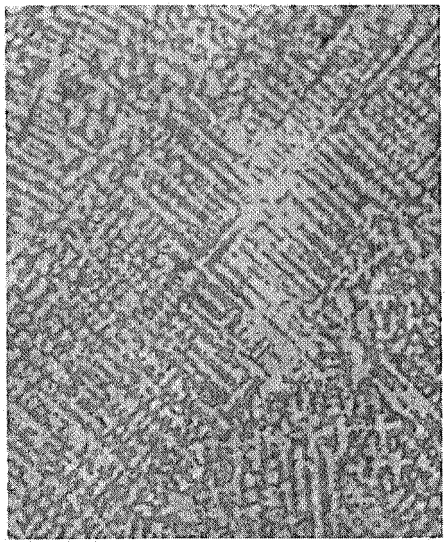

100X

a) As-cast

100X

b) Tested

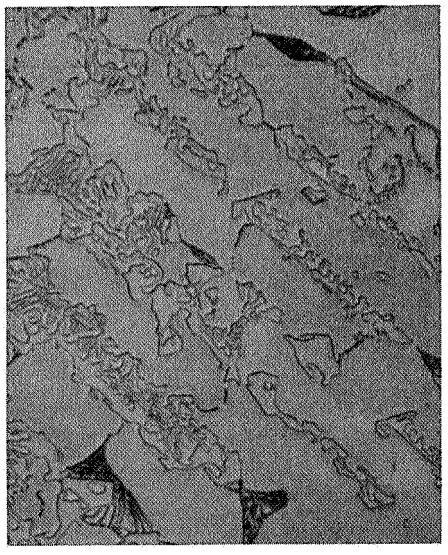

750X

c) As-cast

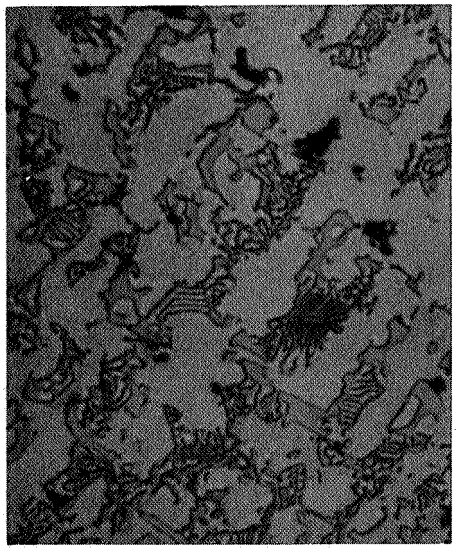

750X

d) Tested

Figure 1. Co-35W-3Cr-0.5C-0.1B, from gage section of stress rupture specimens.

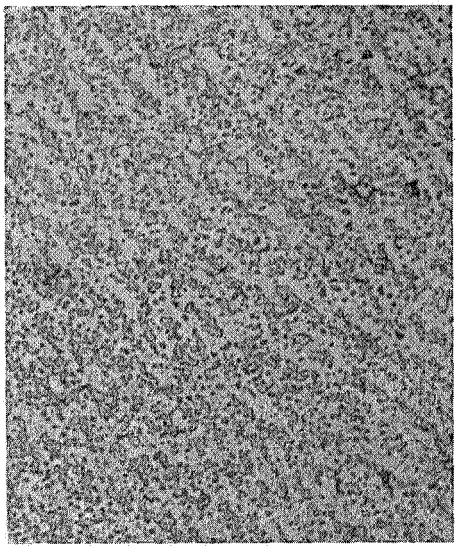

100X

a) As-cast

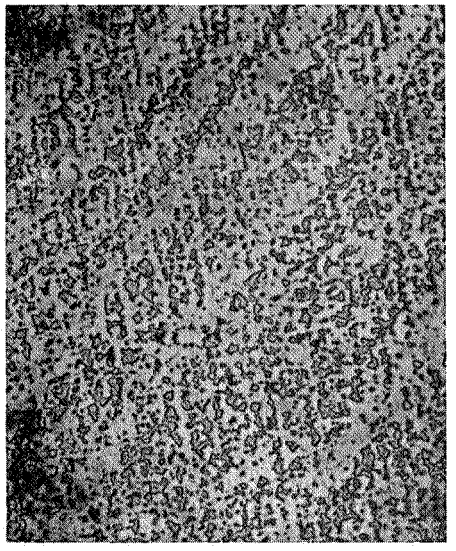

100X

b) Tested

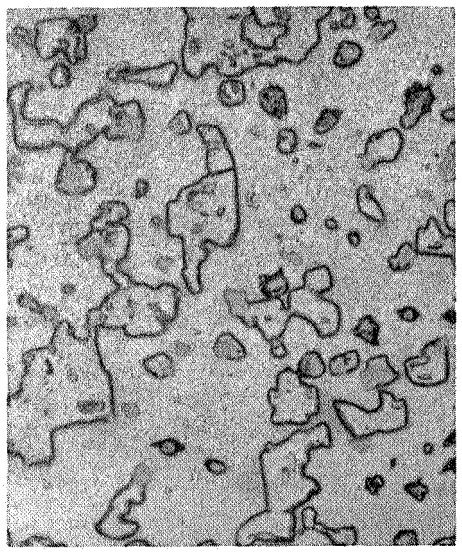

750X

c) As-cast

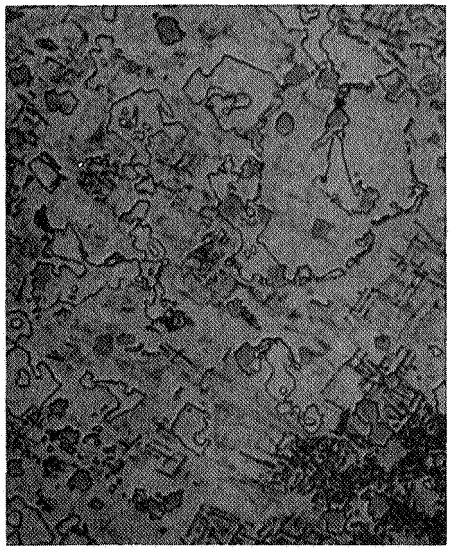

750X

d) Tested

Figure 2. Co-35W-3Cr-2Zr-0.5C-0.1B, from gage section of stress rupture specimens.

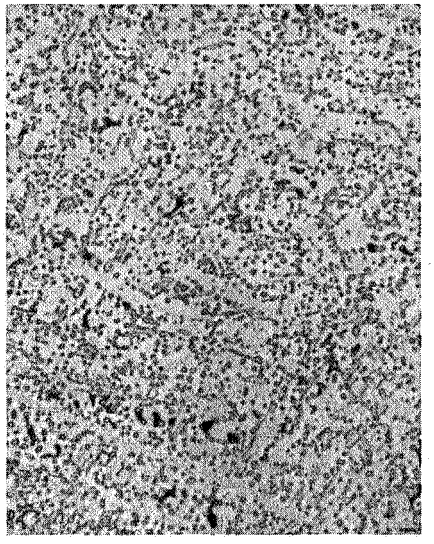

100X

a) As-cast

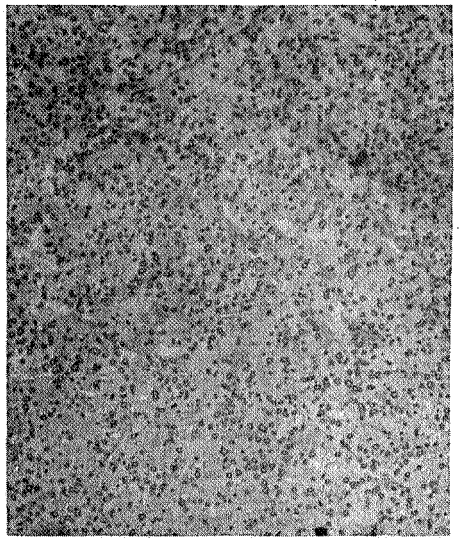

100X

b) Tested

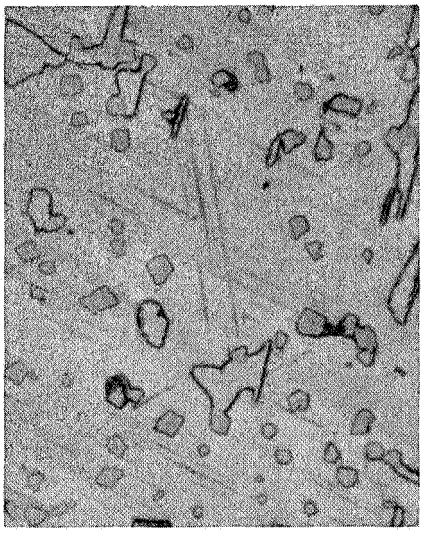

750X

c) As-cast

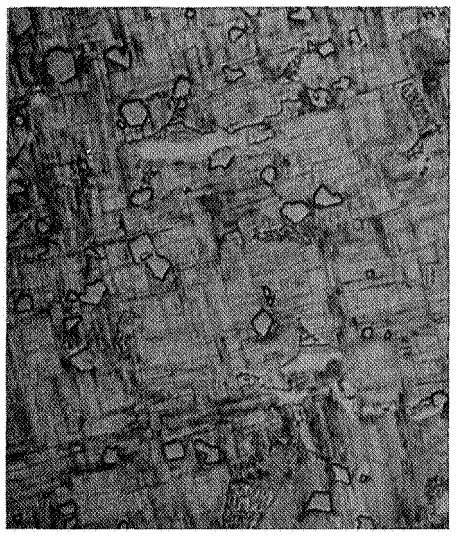

750X

d) Tested

Figure 3. Co-35W-3Cr-2Ti-0.5C-0.1B, from gage section of stress rupture specimens.

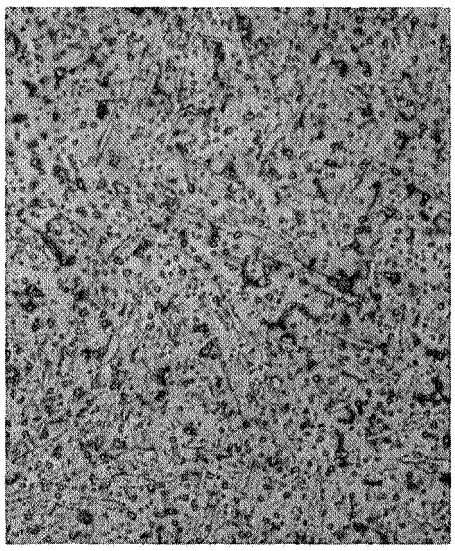

100X

a) As-cast

100X

b) Tested

750X

c) As-cast

750X

d) Tested

Figure 4. Co-35W-3Cr-2Ti-2Zr-0.5C-0.1B, from gage section of stress rupture specimens.

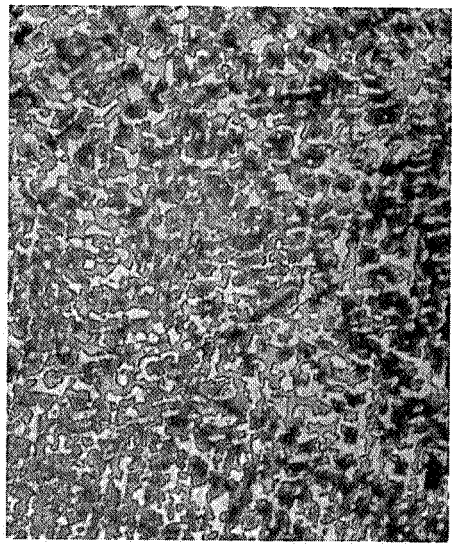

100X

a) As-cast

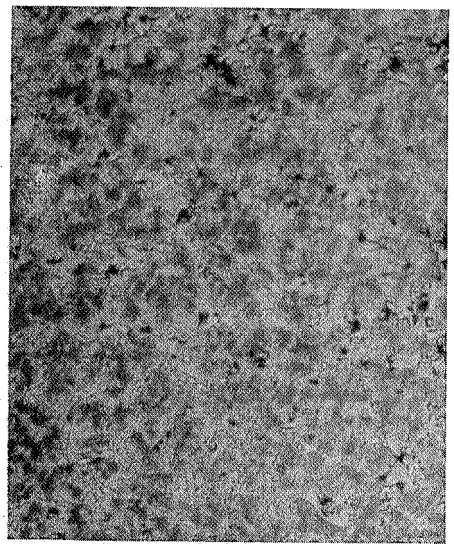

100X

b) Tested

750X

c) As-cast

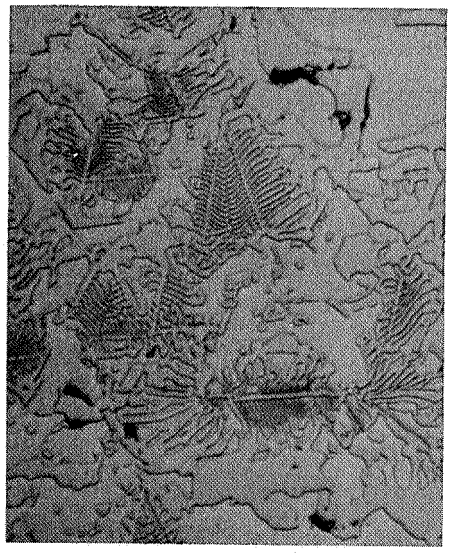

750X

d) Tested

Figure 5. Co-35W-3Cr-1C-0.1B, from gage section of stress rupture specimens.

100X

a) As-cast

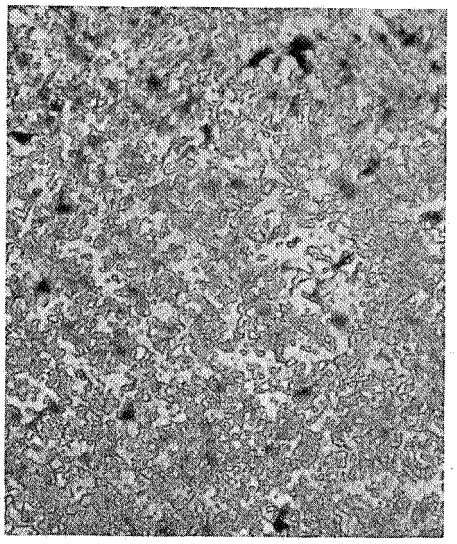

100X

b) Tested

750X

c) As-cast

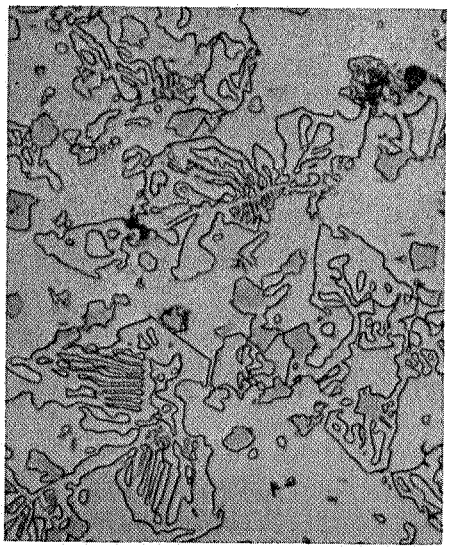

750X

d) Tested

Figure 6. Co-35W-3Cr-2Zr-1C-0.1B, from gage section of stress rupture specimens.

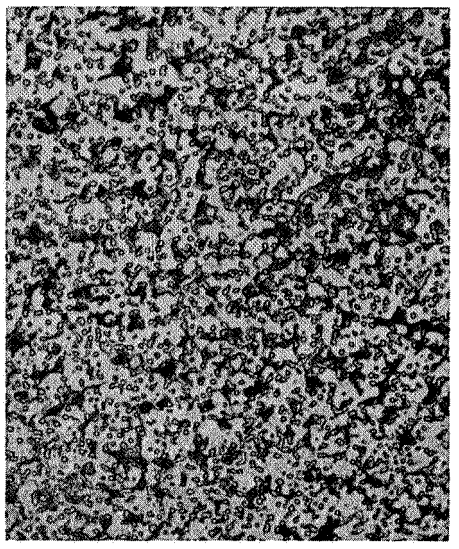

100X

a) As-cast

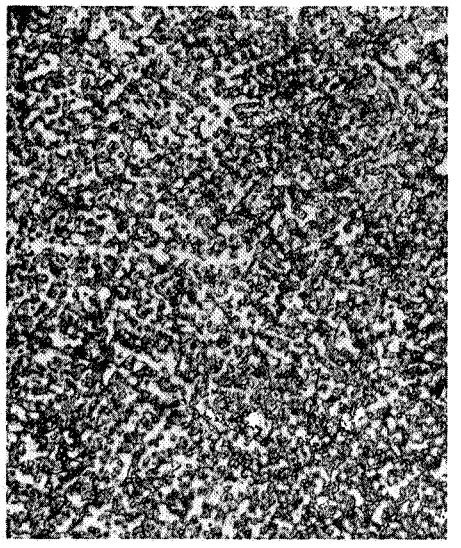

100X

b) After-testing

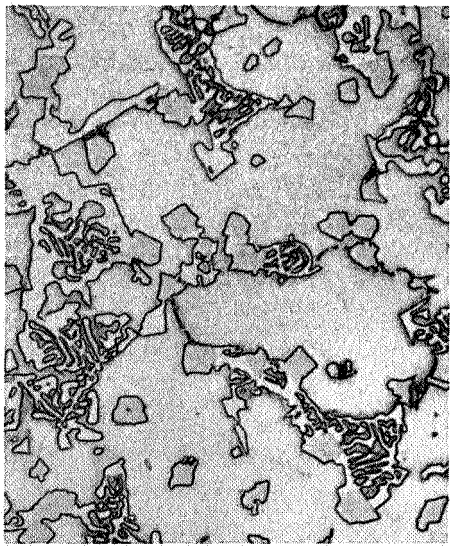

750X

c) As-cast

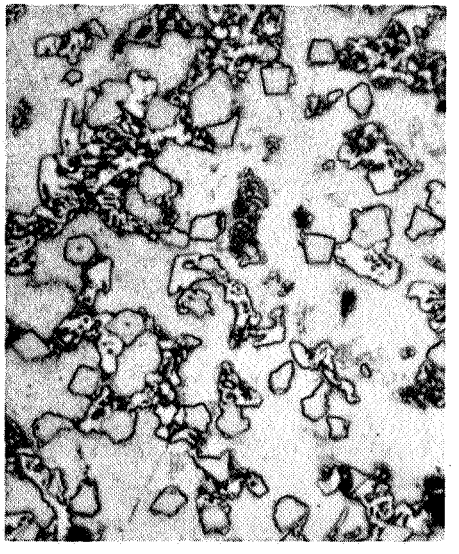

750X

d) After-testing

Figure 7. Co-35W-3Cr-2Ti-1C-0.1B, from gage section of stress rupture specimens.

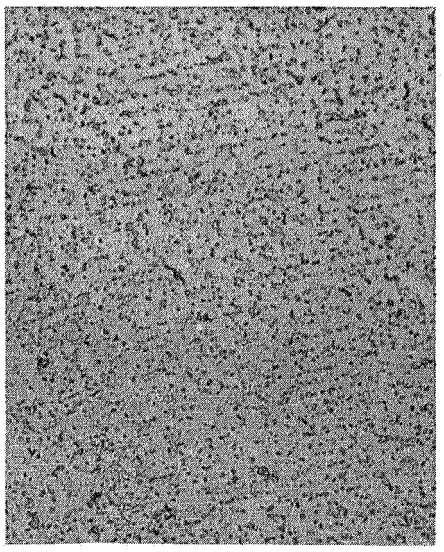

100X

a) As-cast

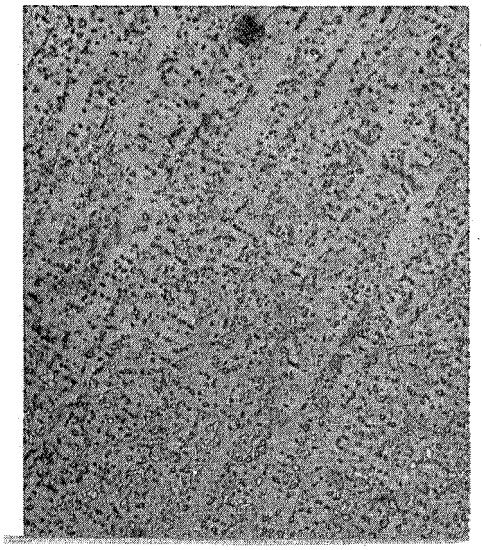

100X

b) After-testing

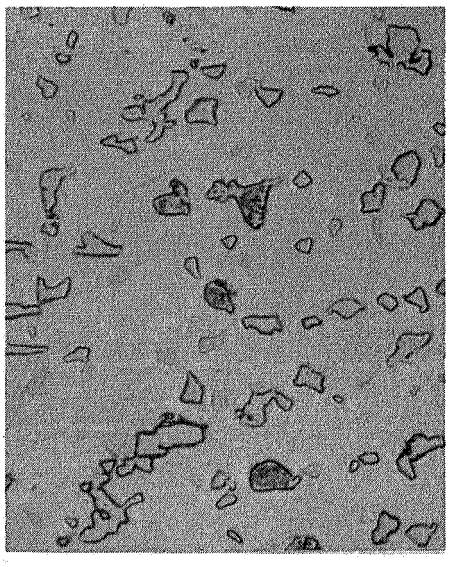

750X

c) As-cast

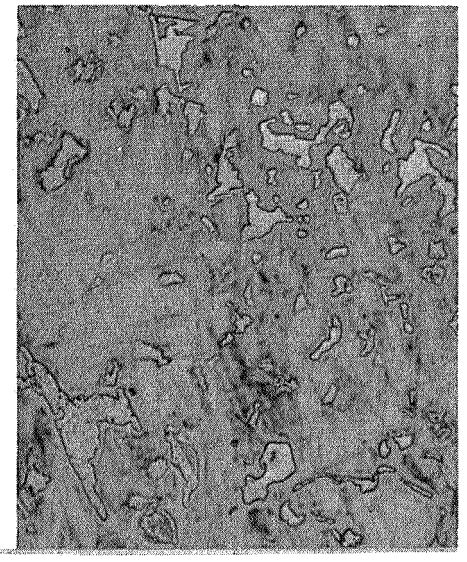

750X

d) After-testing

Figure 8. Co-35W-3Cr-1Ti-1Zr-0.5C-0.1B, from gage section of stress rupture specimens.

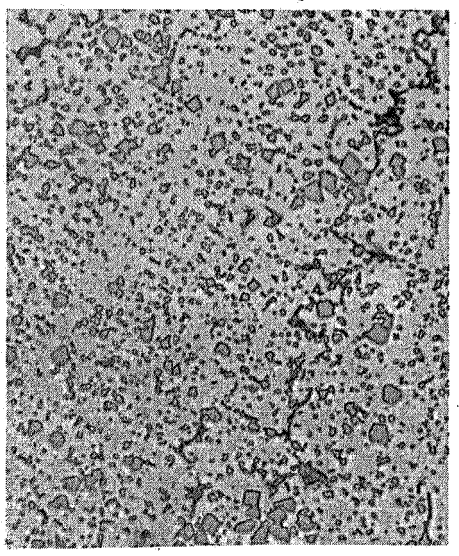

100X

a) As-cast

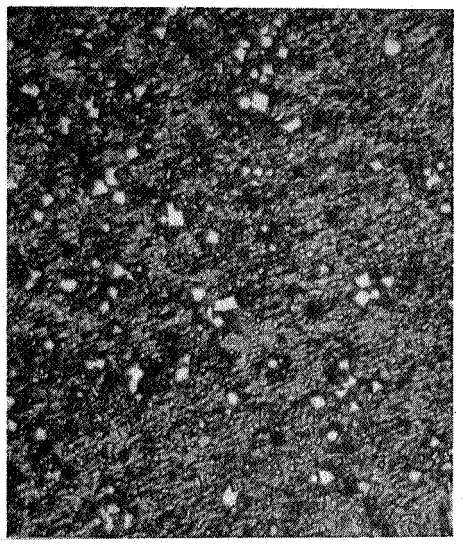

100X

b) After-testing

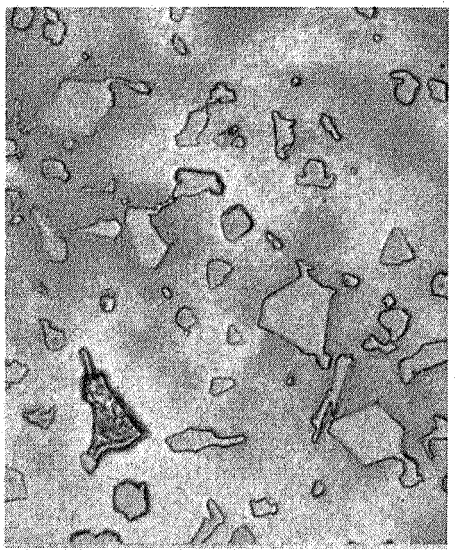

750X

c) As-cast

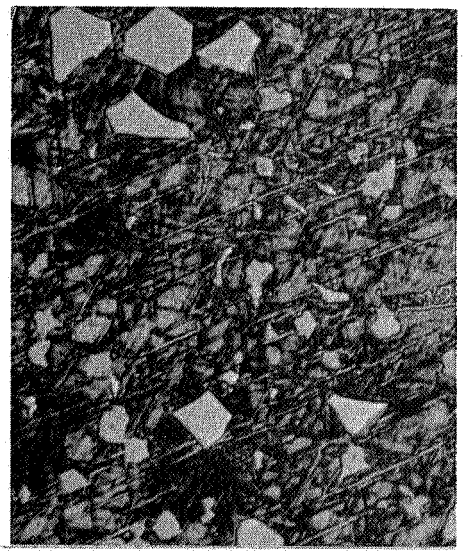

750X

d) After-testing

Figure 9. Co-35W-3Cr-2Ti-2Zr-1C-0.1B, from gage section of stress rupture specimens.

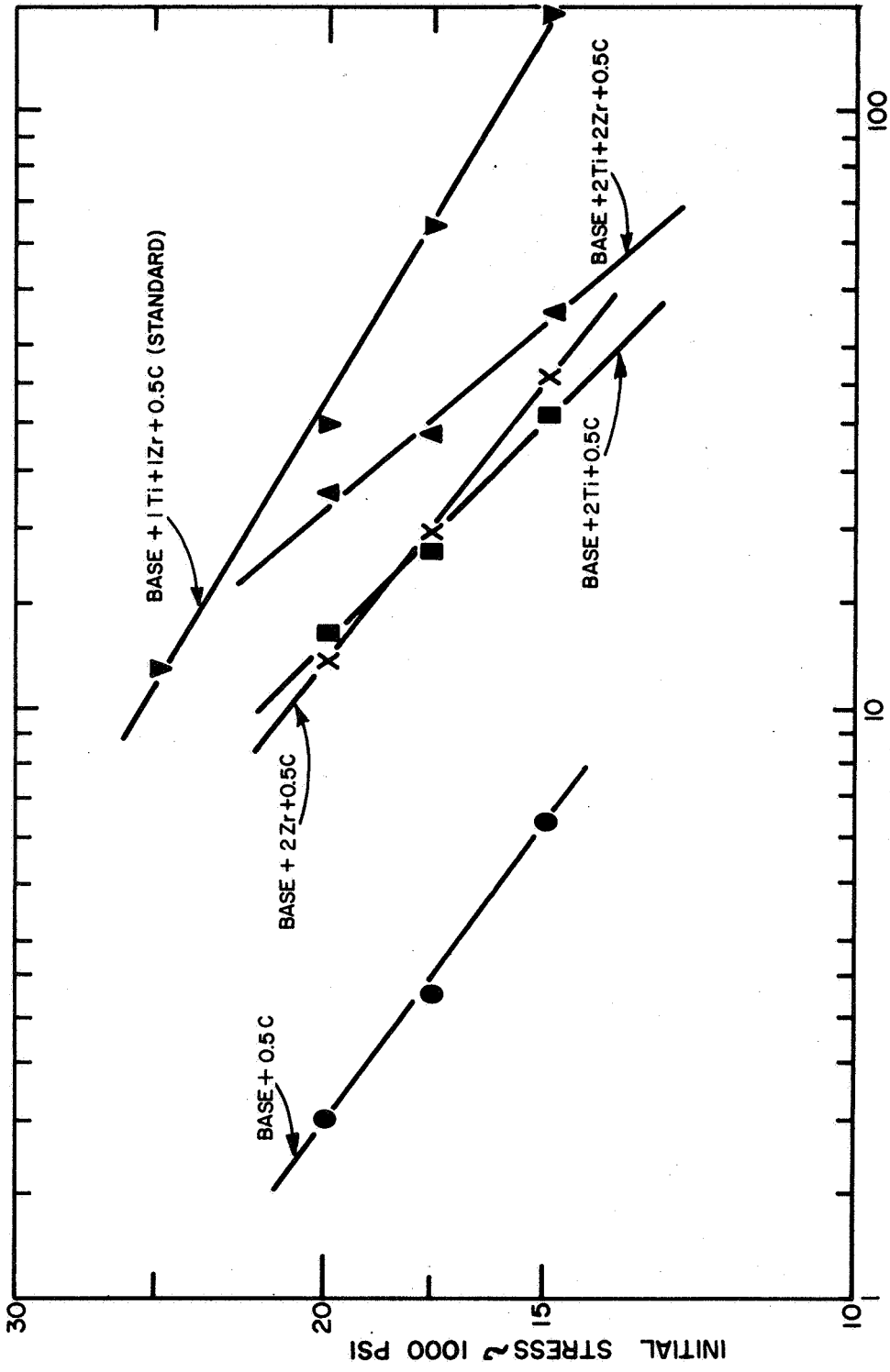

FIG. 10 : EFFECT OF Ti AND Zr ADDITIONS ON A Co – 35W – 3Cr – .5C – 0.1B BASE ALLOY (TESTED AT 1850°F IN AIR).

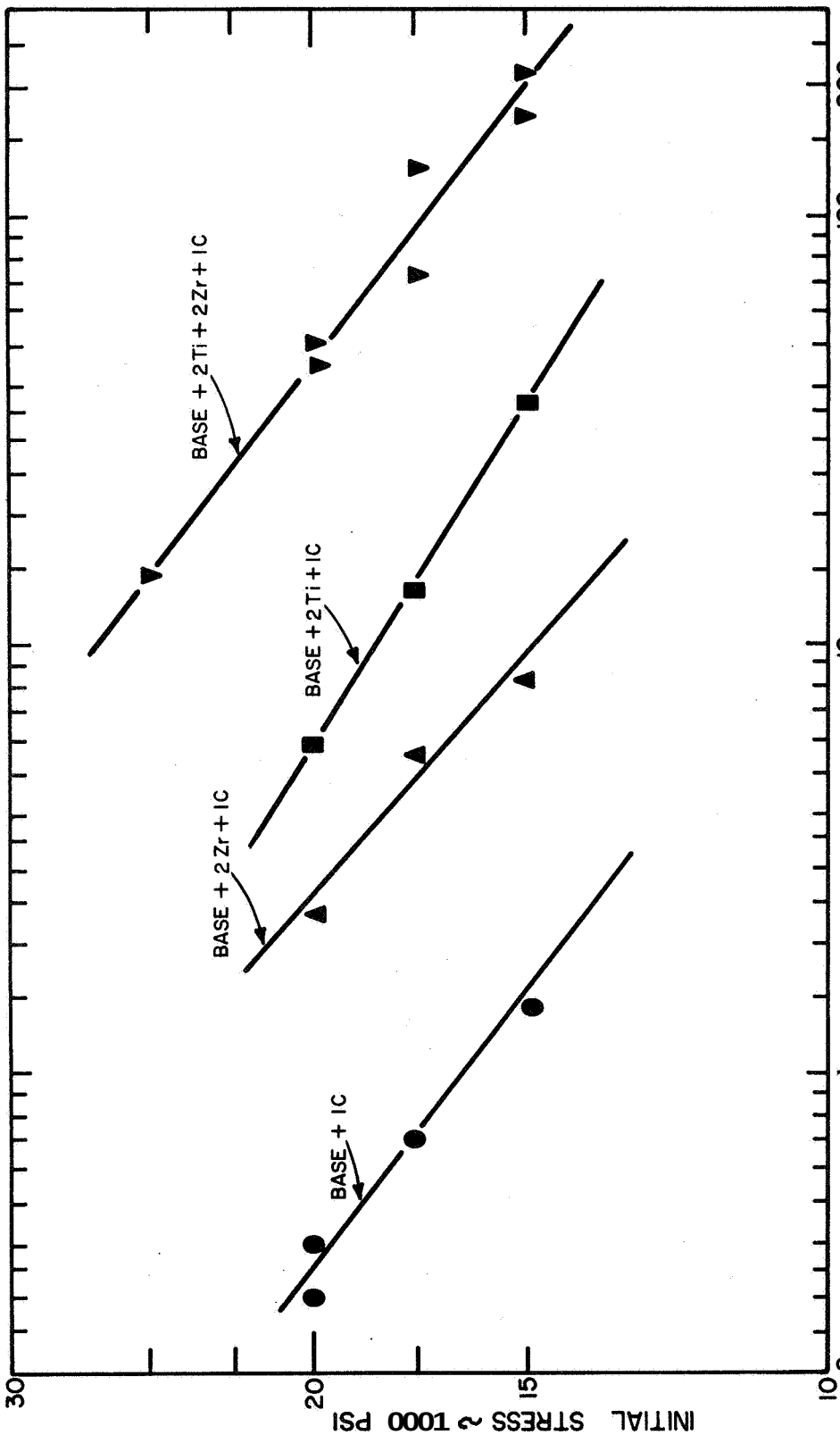

FIG. 11 : EFFECT OF Ti AND Zr ADDITIONS ON A Co-35W-3Cr-1C-0.1B BASE ALLOY (TESTED AT 1850°F IN AIR).

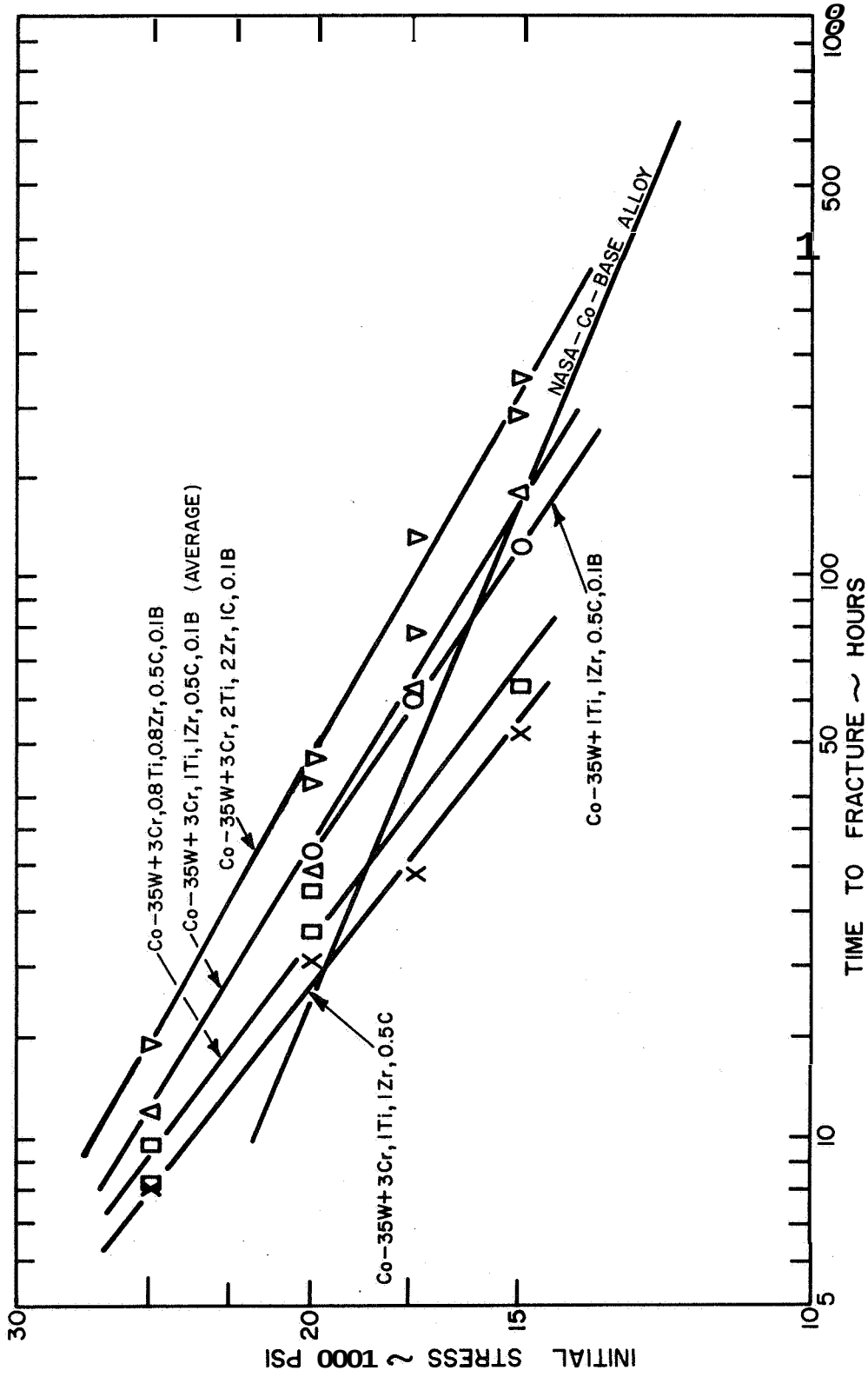

FIG. 12: STRESS-RUPTURE TESTING OF SEVERAL Co-35W BASE ALLOYS. (TESTED AT 1850°F IN AIR)

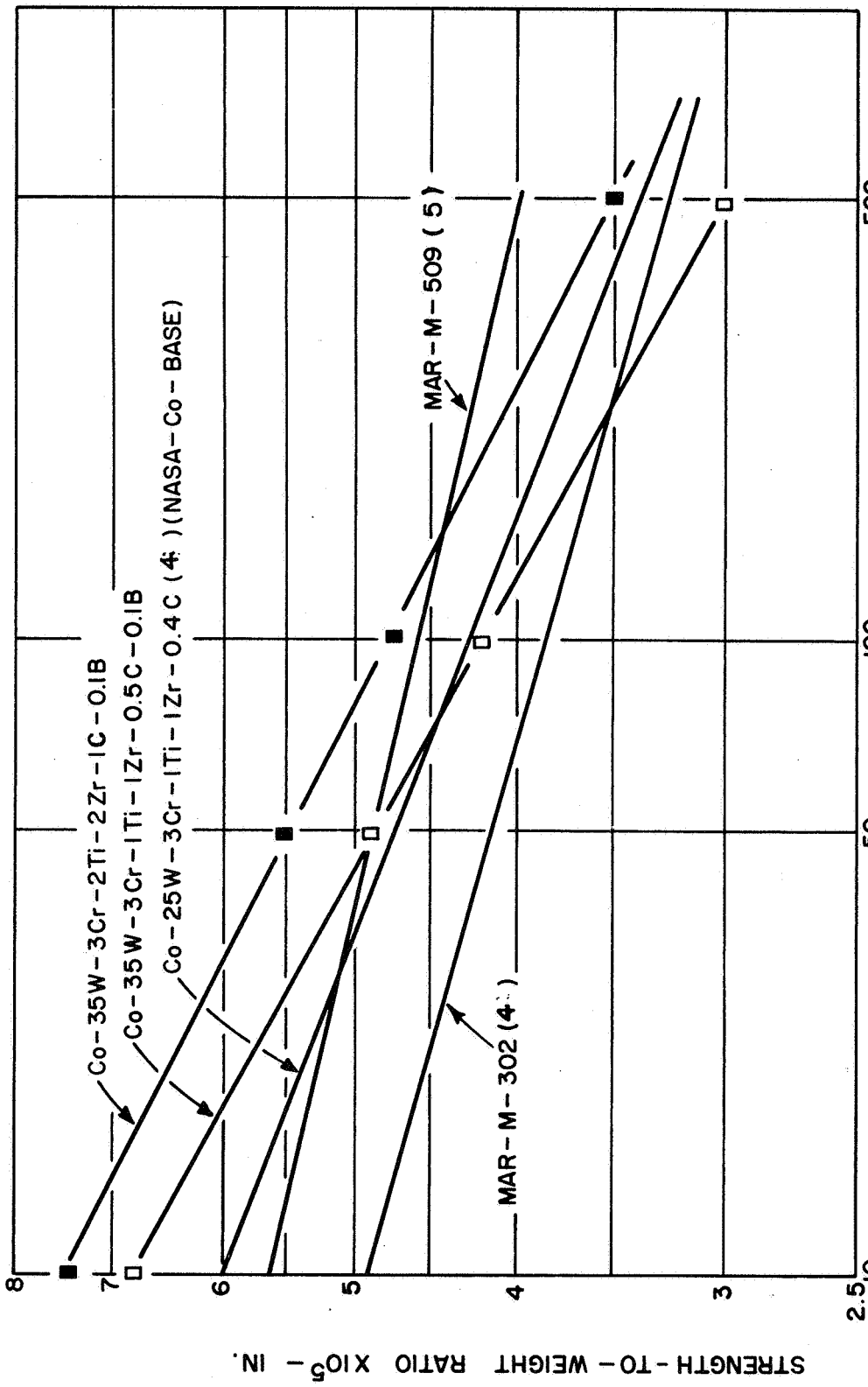

FIGURE 13 : STRESS-RUPTURE PROPERTIES OF SEVERAL Co-BASE SUPERALLOYS ON A STRENGTH-TO-WEIGHT RATIO BASIS.(TESTED AT 1850°F IN AIR)